Pergamon

Energy Convers. Mgmt Vol. 38, No. 18, pp. 1847–1867, 1997
© 1997 Elsevier Science Ltd. All rights reserved
Printed in Great Britain
PII: S0196-8904(96)00112-4
0196-8904/97 $17.00 + 0.00

EFFECTS OF NON-LINEAR PROTECTIVE DEVICES IN CABLE SYSTEMS UNDER ENERGISATION CONDITIONS

NAGAT M. K. ABDEL-GAWAD
Department of Electrical Engineering, Faculty of Engineering, Shoubra, Cairo, Egypt

(Received 26 January 1996)

Abstract—This paper investigates the transient performance of cable systems under energisation conditions, including the non-linear effects of surge divertors which are used as sheath voltage limiters. The method of solution developed and used is based on the modified Fourier transform technique in conjunction with modal analysis. The non-linear effects of surge divertors are included by the use of Duhamel's integral. Mathematical formulations of the transient responses are also given. Both the Cross-bonded and Single-point bonded electrical power cable systems are considered in the study. In the study, the frequency-dependent characteristics of system parameters, in particular skin-effect and effect of the earth-return path, are taken into account in obtaining the transient solutions. Particular attention is given to systems which include cross-bonded cables. The effects of various system parameters, such as source impedance, system length and sheath earthing-resistance, on the transient performance of the systems, as well as on the surge divertor responses, are investigated. © 1997 Elsevier Science Ltd.

Electrical power cable systems Non-linear protective device Switching

1. INTRODUCTION

Transmission systems are usually subjected to overvoltage surges which are dangerous for the system insulation. For the protection of the system against such surges, several means are adopted so as to reduce the overvoltage magnitudes. One such means is to introduce surge divertors, which serve to limit the overvoltages regardless of origin.

As a common philosophy, the utilization of surge divertors has been to protect the terminal apparatus from lightning surges, whereas, as system voltage is increased, switching surges become particularly important compared to lightning surges. Especially on systems operating at 220 kV or above, it has become apparent that surge divertors have been functioning more often on switching surge overvoltages than on lightning discharge overvoltages. For example, it has been reported [1] that, during the first six operating years of the American Electric Power Company's 345 kV system, ordinary switching operations have produced several hundred surge divertor sparkovers. Consequently, there is a real need for studying the performance of the surge divertor and the duty which is imposed upon it each time it operates due to a system switching overvoltage surge. In this study, the performance of the divertors in cable systems under switching conditions is studied rather than their selection which has been studied elsewhere [2].

At present, surge divertors are used as the second line of defense, i.e. they would operate in the case when the other means of protection, such as shunt reactors, pre-insertion resistors, and so on, fail to function properly. On the other hand, it has been reported [3] that, for system voltages of 765 kV, surge divertors are to be used for the control of switching surges, i.e. they will be used as a first line of defense by being operated at almost every system switching overvoltage.

In many studies, the performance of surge divertors against overvoltage surges is handled to some extent both by digital computer [4–8] and T.N.A. [5, 9–11]. However, in this study, mostly single surge divertor operations are considered. Although the operation of three-phase surge divertors in overhead line systems has been considered to some extent [5], simultaneous divertor operations have not been considered in detail. In the present studies, simultaneous surge divertor

operations are studied both in detail and in three-phase cable systems. Inclusion of the frequency dependent characteristics of the cable parameters accurately in obtaining the response of the surge divertors is another contribution presented by these studies. Moreover, introducing the recently developed gapless surge divertors [12–16] in the three-phase cable systems and the study of their behaviour against switching surges using the convolution approach (as convolution integral) in conjunction with the modified Fourier transform method may also be regarded as a contributory work.

In a transmission system, there is a definite source of overvoltages which is the open end of the overhead line or cable where the doubling effect takes place. At these points, the magnitudes of the overvoltages may be controlled by placing surge divertors there. So, in the studies presented here, the effects of the surge divertors are investigated when they are placed at the open receiving-ends of cable systems. Overvoltage surges are produced either by single-phase unit step energisation or by three-phase simultaneous energisation, assuming no trapped charge present and no load current flowing through the system under consideration. Although such switching surge overvoltages have longer wavefronts compared to those which are produced by lightning, surge divertors are capable of dealing with the energies of long duration waves.

The method of solution adopted here to include the non-linear effects of surge divertors is the modified Fourier transform method in conjunction with the Duhamel integral. The method of approach is also verified, giving very good agreement with the results presented by previous work [16].

The non-linear characteristics of the conventional active-gap and gapless surge divertors, which are considered in the studies, are as given in the following sections.

Operations of the surge divertors affect the magnitudes and the shapes of the subsequent switching surges. The overvoltages produced in the system are modified under the influence of the divertor characteristics and system parameters, such as short circuit power of the source, length of the transmission system, sheath earthing-resistance of the cables and cable type. Therefore, the effects of these factors are all investigated.

2. THE METHOD OF SOLUTION

The basic approach to include a non-linear element in a system involves the application of convolution. Namely, once the system response to a unit step function is known across the points where the non-linear element is connected, the response of the system to a general excitation can be determined through the use of the Duhamel integral which is a version of the convolution. So, in determining the response of a non-linear element, the required information is the unit-step response and the open-circuit voltage of the system across the points to which the non-linear element is connected. The unit step response, as a voltage waveform, may be obtained by injecting a unit step current at the terminals of the non-linear element. Before the current injection, the non-linear element is removed from its terminals, and the system is made passive by making all sources equal to zero. Again ignoring the presence of the non-linear element, the open-circuit voltage across its terminals is calculated taking into account the system conditions and disturbances, such as switching operations, faults, etc. Both the unit step response and the open-circuit voltage of the system are determined using the modified Fourier transform method. The waveforms, thus obtained, are then coupled with the Duhamel integral in the time domain to yield the response of the non-linear element during the period of current flow through it. The current flow for a gapless surge divertor may be assumed to be continuous for all elements. However, this is not the case for a conventional surge divertor due to the presence of the spark-gaps in series with the non-linear resistor in it. The current through a conventional surge divertor starts flowing immediately following the sparkover and is extinguished after a certain time. Thus, its operation may be considered as a switching operation, and its effect on the system transients continues also after the divertor is switched out of the circuit. This effect is determined by injecting the divertor current through the terminals of the surge divertor using the piecewise Fourier transform method [17]. The injection is accomplished by ignoring the presence of the surge divertor and making the system passive. The transient voltage appearing across the surge divertor terminals

due to this injected current is added to the steady-state voltage across the terminals of the divertor, ignoring its presence. Thus, the modified voltage waveform across the conventional surge divertor is obtained with the divertor being switched out of circuit.

2.1. Duhamel's integral

The response $g(t)$ of a system, which is initially passive, to an input signal $f(t)$ can be expressed by the convolution [18] of $f(t)$ and the unit response $k(t)$, i.e.

$$g(t) = f(t)*k(t)$$

$$= \int_0^t f(t-\tau)k(\tau)\mathrm{d}\tau \tag{1}$$

where the asterisk, *, denotes the convolution and $f(t) = 0$ for $t < 0$. In power engineering, it is more common to employ the unit step response rather than its formal derivative, which is the impulse response. Considering a unit step response $TF(t)$, the corresponding impulse response function $k(t)$ may be given by,

$$k(t) = \frac{\mathrm{d}}{\mathrm{d}t} TF(t) + TF(0)\delta(t) \tag{2}$$

where $TF(t) = 0$ for $t < 0$ and $\delta(t)$ is the Dirac delta function [60]. Substituting equation (2) into equation (1) yields,

$$g(t) = f(t)TF(0) + f(t)* \frac{\mathrm{d}}{\mathrm{d}t} TF(t) \tag{3}$$

or

$$g(t) = f(t)TF(0) + \int_0^t f(t-\tau)TF'(t-\tau)\mathrm{d}\tau \tag{4}$$

which can also be given as:

$$g(t) = f(0)TF(t) + \int_0^t TF(t-\tau)f'(\tau)\mathrm{d}\tau \tag{5}$$

where the prime denotes differentiation with respect to time. Equations (4) and (5) are known as Duhamel's formulae or integrals [19–23]. They serve to express the response of a system to a general driving function $f(t)$, making use of the system response to a unit step function. Duhamel's integrals have been used successfully to solve the transient problems arising in power systems. Writing equation (5) in numerical form gives:

$$g(t) = f(0)TF(t) + \int_{k=1}^{n} TF(t - k.\Delta\tau).\Delta f \tag{6}$$

where $\Delta f = \{f(k.\Delta\tau) - f((k-1).\Delta\tau)\}$ and $n = t/\Delta\tau$ and t is the time at which the output is required. Equation (6) is used in the numerical evaluation of Duhamel's integral.

3. VERIFICATION OF THE APPROACH TO INCLUDE THE EFFECT OF SURGE DIVERTORS

The method of approach to include the non-linearity due to the operation of surge divertors is as given in the following section. The method used is verified for a maximum frequency of

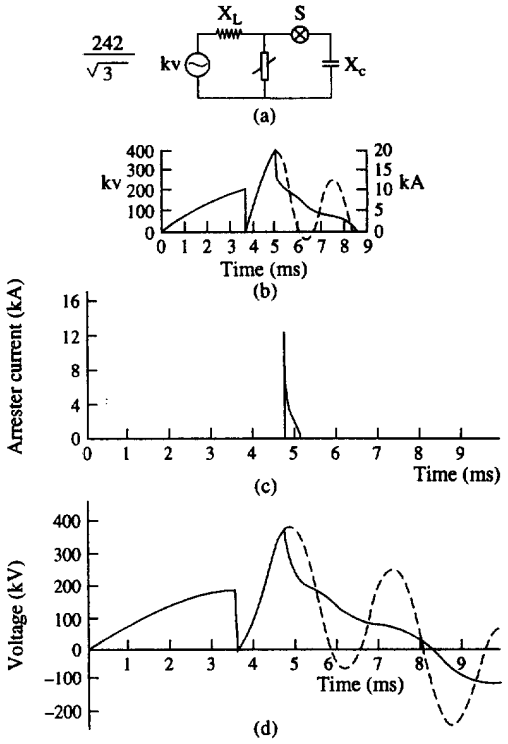

Fig. 1. Operation of conventional active-gap surge divertor. (a) Circuit diagram. (b) Results from ref. [16]. (c) Computed current of the surge divertor. (d) Computed voltages across the surge divertor.

12,500 Hz, using the circuit in Fig. 1a and the results are then compared with those given by Ref. [16].

The circuit shown in Fig. 1a, given in Ref. [16], represents the energisation of a 135 Myar capacitor bank through a switch S. The capacitor is protected by a divertor which starts operating when the capacitor is charged to the sparkover voltage level. The source voltage is $242/\sqrt{3}$ kV (r.m.s.), and the power frequency is 60 Hz. Before the switch closure, the system is under steady-state, and the switch closes at $t = 3.667$ ms. The capacitance of the capacitor bank is 6.667 μf, and the source inductance is 0.0247 henry. The parameters of the conventional surge divertor are: $k = 35{,}100$ and $\beta = 0.25$ which refer to the constants in the voltage-current equation of the non-linear resistor elements, i.e. in $v = kI^{\beta}$, where v and I are in volts and amperes, respectively. Sparkover voltage of the divertor is 382 kV. The parameters of the active gap characteristic are such that the ceiling value of the gap voltage is 0.7 pu of the divertor rating, i.e. 178.19 kV, and $T_1 = 0.32$ ms and $T_2 = 0.5$ ms.

The parameters of the gapless surge divertor are: $k = 246830$ and $\beta = 0.0385$ in the equation of $v = KI^{\beta}$, where v and I are volts and amperes, respectively.

Figures 1 and 2 illustrate the voltage and current waveforms due to the operations of conventional and gapless surge divertors, respectively. The results shown by Figs. 1b and 2b from Ref. [16] are for comparison. The prospective voltage, i.e. the voltage which would appear across the divertor terminals if the divertor were not present, is shown by dashed lines. The peak current drawn by the conventional divertor has been computed to be 12.413 kA in Fig. 1c, whereas the gapless surge divertor, which has no arc gaps in series with its zinc oxide valve elements, has drawn a much lower peak current of 1.97 kA as shown in Fig. 2c. The corresponding peak currents in Ref. [16] are 12.4 kA and 1.8 kA, respectively.

Consequently, the voltage and current waveforms and peak values obtained as a result of the surge divertor operations are in good agreement with those given in Ref. [16].

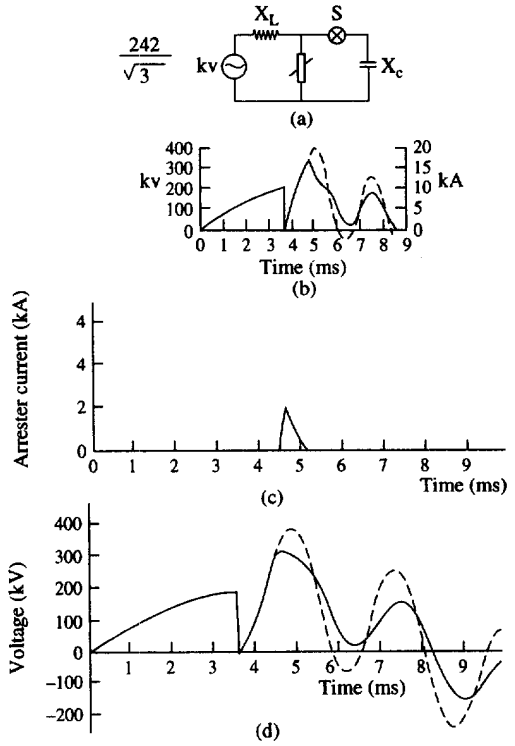

Fig. 2. Operation of gapless surge divertor. (a) Circuit diagram. (b) Results from ref. [16]. (c) Computed current of the surge divertor. (d) Computed voltages across the surge divertor.

4. ANALYSIS OF THE CABLE SYSTEM

The cable system considered is a 275 kV three-phase system which consists of three single-core cables. The system studied is either cross-bonded of Kirke-Searing type or single-point bonded type. The sheaths are solidly inter-connected at the terminating ends of the single-point bonded cable or the ends of each major section of the cross-bonded cable. Three-phase surge divertors are connected at the receiving end of the cables as shown by the single-line diagram in Fig. 3, where L_S and L_R are possible shunt reactors to be connected at the sending and receiving end busbars.

The length of the cable is 27.432 km. The cross-bonded cable consists of 20 major sections, i.e. each major section has a length of 1.3716 km. The individual cables of the single-point bonded cable system have the same dimensions as those of the cross-bonded system. They are laid in trefoil formation as illustrated in Fig. 4. The data used for the studies are given in Appendix A. The data related to the individual phase cables is given in Table A.1. The modal parameters of the cross-bonded and single-point bonded cables are given by Tables A.2 and A.3, respectively, in which the order of the elements of the characteristic impedance and admittance matrices, as well as the order of the voltage and current eigen vectors arising, refer to the middle, right hand side and left hand side cable conductors, respectively. The earth resistivity is taken to be 20 Ω-m in this system.

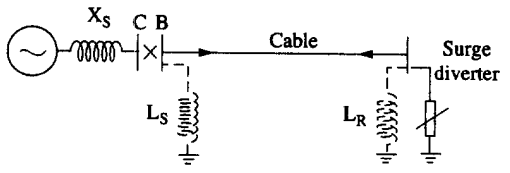

Fig. 3. Single-line diagram of the 275 kV cable system with surge divertor at the receiving end.

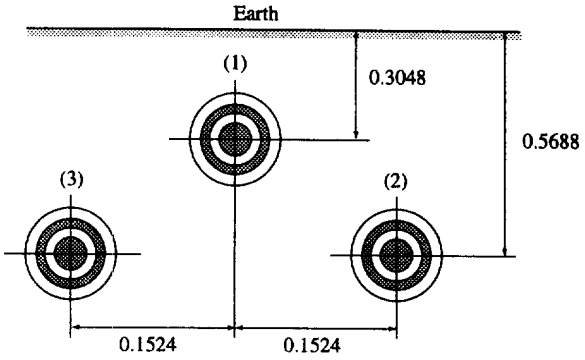

Fig. 4. Configuration of the 275 kV cable system (in meters).

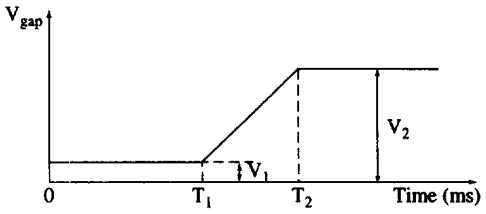

Fig. 5. Volt-time characteristic of a conventional active gap.

4.1. Characteristics of the surge divertors

Two types of divertors are considered in the studies, namely conventional active gap and gapless surge divertors. The gap characteristic of the conventional divertor is illustrated by Fig. 5. The voltage–current characteristic of the non-linear resistors of both types of divertors, however, is expressed by $v = KI^{\beta}$, where v and I are in volts and amps, respectively. For the 275 kV cable system, the parameters K and β of the individual divertors and the data of the gap characteristic of the conventional divertor are the same as given above earlier.

5. MATHEMATICAL FORMULATIONS TO OBTAIN THE PERFORMANCE OF SURGE DIVERTORS

The response of a surge divertor against overvoltages can be obtained by using the Duhamel integral which requires the unit step response and the open-circuit voltage of the system across the points of the surge divertor terminals. These will be formulated below.

5.1. Open-circuit voltage of the cable system

The cable system shown in Fig. 3 may be represented by the equivalent block diagram in Fig. 6, with the surge divertors being removed from the receiving end.

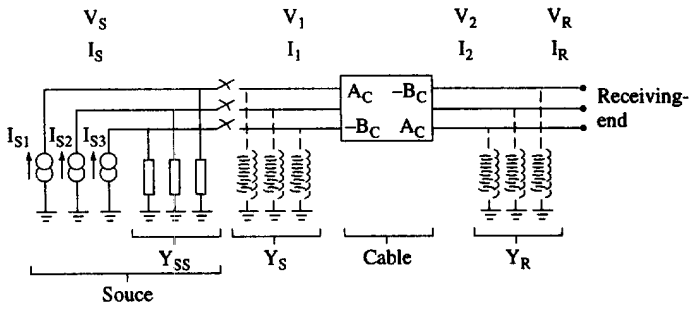

Fig. 6. Equivalent diagram of the cable system of Fig. 3 (cable sheaths solidly earthed).

The terminal voltages and currents of the cable may be related by the two-port matrix equation as:

$$\begin{vmatrix} \mathbf{I}_1 \\ \mathbf{I}_2 \end{vmatrix} = \begin{vmatrix} A_C & -B_C \\ -B_C & A_C \end{vmatrix} \begin{vmatrix} \mathbf{U}_1 \\ \mathbf{U}_2 \end{vmatrix} \tag{7}$$

where A_C and B_C are the reduced nodal matrices of the cable. Including the admittance matrices of the sending end and receiving end shunt reactors and that of the source, i.e. Y_S, Y_R and Y_{SS}, respectively, and also taking the receiving end current as zero, equation (7) is modified as:

$$\begin{vmatrix} \mathbf{I}_S \\ 0 \end{vmatrix} = \begin{vmatrix} A_C + Y_S + Y_{SS} & -B_C \\ -B_C & A_C + Y_R \end{vmatrix} \begin{vmatrix} \mathbf{U}_S \\ \mathbf{U}_R \end{vmatrix} \tag{8}$$

where Y_S, Y_R and Y_{SS} are all diagonal matrices. If the cable sheaths are earthed through resistors, A_C will have an order of 4×4, hence the diagonal matrices Y_S, Y_R and Y_{SS} may be considered to have orders of 4×4, with the last diagonal element being zero. If there are no shunt reactors at any ends, the terms Y_S and/or Y_R will be zero. $\mathbf{U}_S$ and $\mathbf{U}_R$ are the sending and receiving end voltage vectors and $\mathbf{I}_S$ represents the sending end currents generated by the current source. The voltage vector $\mathbf{V}_R$, which corresponds to the open-circuit voltages across the terminals of the surge divertors, can be derived from equation (8) yielding:

$$\mathbf{U}_R = (A_C + Y_R)^{-1} B_C Z_{in} * \mathbf{I}_S \tag{9}$$

where

$$Z_{in} = (\{A_C + Y_S + Y_{SS}\} - B_C\{A_C + Y_R\}^{-1} B_C)^{-1}$$

5.2. *Unit step responses*

Unit step responses are obtained as voltage waves by injecting unit step currents at the terminals of the surge divertors, with the divertors being removed from their terminals and the system being made passive, i.e. all sources are made zero. Mathematical formulations of the unit step responses will be formulated below for the cable system considered.

Considering the cable system illustrated by the circuit diagram in Fig. 6, when the sources are all made zero and possible shunt reactors are included in the cable's two-port matrix equation, the diagram may be represented as in Fig. 7, with the unit step currents being injected in turn, from the surge divertor terminals. The unit step responses due to the subsequent injections of the

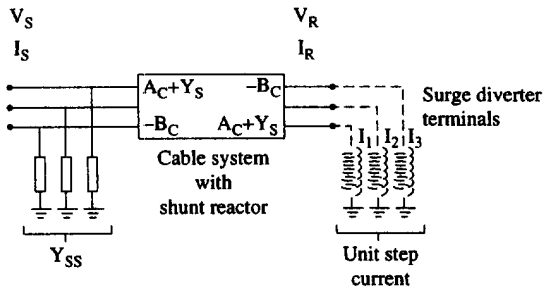

Fig. 7. Passive cable system of Fig. 6 with the unit step currents being injected from the surge divertor terminals.

unit step currents are obtained in matrix form. Letting (TF) represent such a matrix, it may be expressed by:

$$(TF) = Z_{in} \begin{vmatrix} I_1 & 0 & 0 \\ 0 & I_2 & 0 \\ 0 & 0 & I_3 \end{vmatrix} \tag{10}$$

where I_1, I_2 and I_3 are unit step currents, and Z_{in} is the input impedance matrix of the system from the surge divertor terminals of Fig. 7.

The two-port matrix equation of the system shown in Fig. 7 may be written as:

$$\begin{vmatrix} \mathbf{I}_S \\ \mathbf{I}_R \end{vmatrix} = \begin{vmatrix} A_C + Y_S + Y_{SS} & -B_C \\ -B_C & A_C + Y_R \end{vmatrix} \begin{vmatrix} \mathbf{U}_S \\ \mathbf{U}_R \end{vmatrix} \tag{11}$$

where $\mathbf{I}_S = 0$; Y_S and Y_R are the diagonal admittance matrices of the sending and receiving end shunt reactors and Y_{SS} is the source admittance matrix. The input impedance matrix Z_{in} may be derived from the equation which expresses the receiving end voltage $\mathbf{U}_R$ in terms of the current $\mathbf{I}_R$, i.e. from equation (11). It can be written that:

$$\mathbf{U}_R = Z_{in} * \mathbf{I}_R \tag{12}$$

where

$$Z_{in} = (\{A_C + Y_R\} - B_C\{A_C + Y_S + Y_{SS}\}^{-1}B_C)^{-1}$$

Substituting Z_{in} in equation (10) yields the unit step responses matrix (TF).

6. SYSTEM STUDIES

The performance of the surge divertors, using a digital computer, is presented. Overvoltages are produced by switching operations to energise the system under study. The effects of several factors on the response of the surge divertors are investigated. For example, the effects of source impedance, cable length and type, sheath earthing-resistance and the type of the surge divertors are studied.

It is assumed that the surge divertor employed maintains the spark-over voltage level also after subsequent sparkovers. Besides this, the voltage drop in the connecting leads, which are made as short as possible in practice, is assumed to be zero.

The single-line diagram of the cable system to be studied is shown in Fig. 3. The system is of 275 kV, and the data of the cable conductors are given in Appendix A. The characteristics of the surge divertors have been described. Three-phase surge divertors are placed at the receiving end. First, single-phase and then three-phase energisations are considered as being the origins of the overvoltages.

6.1. Response of surge divertors due to single-phase energisation

The cable system shown in Fig. 3 is energised by a unit step voltage from the first conductor which is the middle conductor of the system. The unit step voltage is applied between the phase conductor and earth. This type of energisation might also simulate a lightning strike to a phase conductor. No compensation and no trapped charges are assumed to be present on the system. Energisation takes place from an infinite busbar. Cable sheaths are solidly earthed at the terminating ends as well as at the major section joints of the cross-bonded cable. Both cross-bonded and single-point bonded types of cables are considered. In order to see the effect of divertor operation clearly, the voltages appearing at the receiving end with and without the presence of the surge divertors are obtained and compared with each other.

Figure 8 ($L = 27.432$ km) shows the responses of conventional active-gap surge divertors when they are placed at the receiving end of a cross-bonded cable. If the presence of the divertors is ignored, then the voltage waveforms at the receiving end will have the form shown in Fig. 8c. Figure 9 also shows the same waveforms but for an observation time of 2 ms. The induced voltages

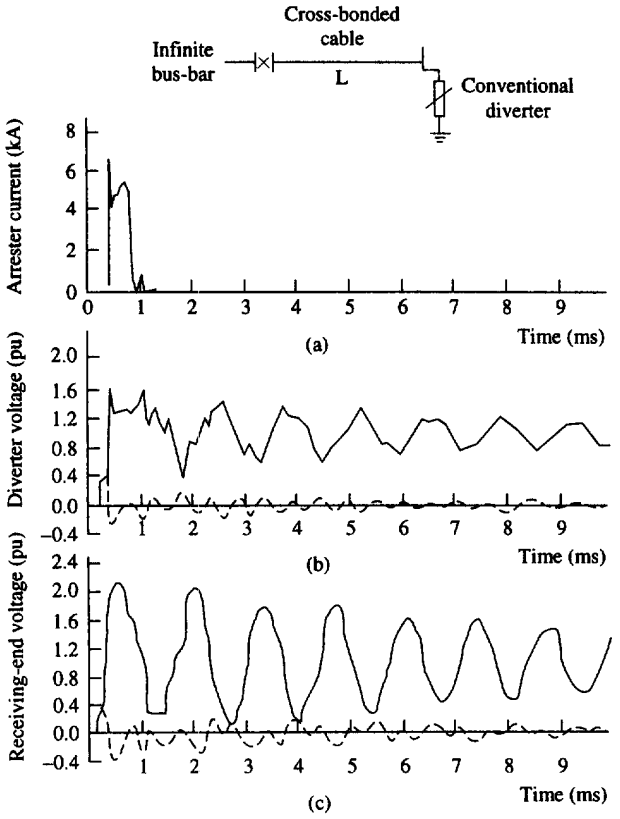

Fig. 8. The effect of surge divertor operation due to single-phase, unit step energisation of cross-bonded cable (observation time = 10 ms). (a),(b) Response of the surge divertor, (c) receiving end voltages (no divertors). ___ energised phase (phase 1); – – – unenergised phases.

on the unenergised cores 2 and 3 have identical waveforms, as can be seen in Figs 8c and 9c, because of the symmetric configuration of the trefoil arrangement. Also, in these figures, the doubling effect of the voltages at the open-circuited cable end is observed on the receiving end voltage waveform of the energised core.

The surge divertor starts operating when the voltage across it exceeds its sparkover voltage. Although, at the receiving end, there is a divertor between each phase conductor and earth, only one of them, which is connected to the energised phase, is seen to be operating. The operation of the divertor modifies the voltages appearing at the receiving end, as can be seen in Figs 8b and 9b. After the sparkover of the divertor, the voltage across the surge divertor terminals drops and remains low enough not to cause any discharges in the system insulation. As a result of the divertor operation, the voltage oscillations at the receiving end die out quickly. On the other hand, the induced voltages on the unenergised cores are also modified slightly. The divertor current which flows through the operated surge divertor is shown in Figs 8a and 9a. It rises quite sharply when the divertor sparks over and reaches a value of about 6 kV. The divertor current rises to such a high value because of the considerable capacitive effect and low surge impedance of the cables. Hence, severe discharge duty is imposed upon the divertor being operated.

Figures 10 and 11 show the waveforms in the case of the single-point bonded cable, for observation times of 10 ms and 2 ms, respectively. If the divertor responses are compared with those of Figs 8 and 9, it is seen that, in the case of the single-point bonded cable, the divertor voltage, after sparkover, comes to the steady-state value much more rapidly, and the divertor current reaches a value of about 7 kA. This value is a bit higher than the value obtained for the case of the cross-bonded cable because the surge impedance of the single-point bonded cable is less than that of the cross-bonded cable. If the presence of the surge divertors were ignored, the receiving end voltage waveforms would be as shown in Figs 10c and 11c. As shown in Fig. 10c, the voltage

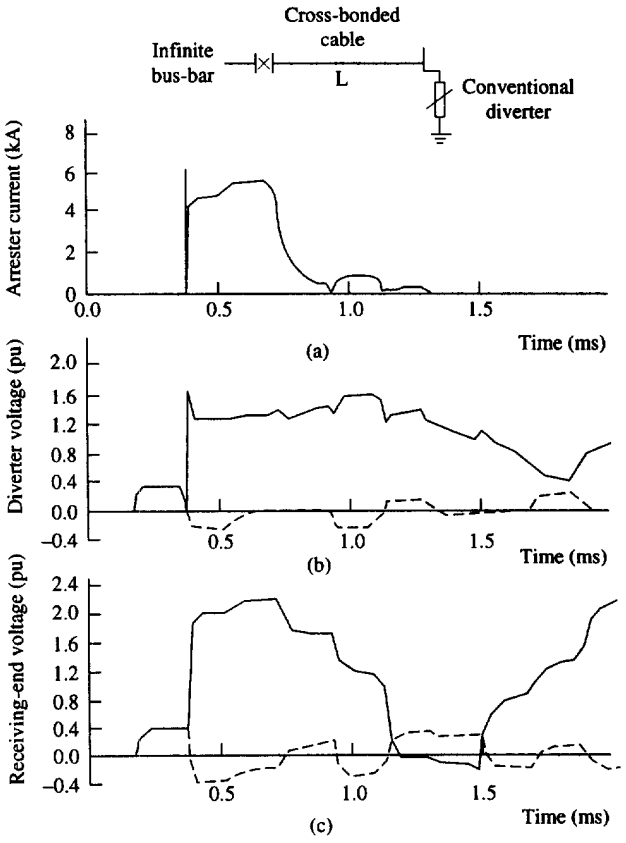

Fig. 9. The effect of surge divertor operation due to single-phase unit step energisation of cross-bonded cable (observation time = 2 ms). (a),(b) Response of the surge divertor, (c) receiving end voltages (no divertors). ____ energised phase (phase 1); – – – unenergised phases.

oscillations at the receiving end of the single-point bonded cable die out much more quickly compared to the case of the cross-bonded cable. This may be explained by the fact that the single-point bonded cable is homogeneous throughout its length, whereas, within each major section of a cross-bonded cable, there exist points of discontinuities at the cross-bonding points of the sheaths.

6.2. Response of surge divertors due to three-phase energisation

In this case, the overvoltages are produced by the three-phase simultaneous energisation of the cable systems. When the energisation takes place, the first phase voltage is assumed to be at its peak value. The responses of the three-phase surge divertors are obtained by studying the effects of several system parameters, as well as the effects of surge divertor type.

6.2.1. Effect of source impedance. The source impedance affects the shapes and the magnitudes of the transient voltages considerably. Therefore, the response of the surge divertors will also be under the influence of the source impedance. This will be illustrated by various source conditions. In these studies, the sheaths of the cross-bonded cable to be considered are solidly earthed at the ends of each major section. The responses are obtained for an observation time of 10 ms, considering a maximum frequency harmonic of 15 kHz.

Figure 12 shows the response of active-gap conventional surge divertors for the case of an infinite busbar source (for cross-bonded cable). If the divertor were not present, the voltage at the divertor location would reach a value of almost 2 pu, as shown in Fig. 12c. If the divertor is present, it does not let the voltage, at its terminals, rise to that value. However, it sparks over at the sparkover voltage, causing the voltage at the divertor location to be modified, as can be seen in Fig. 12b.

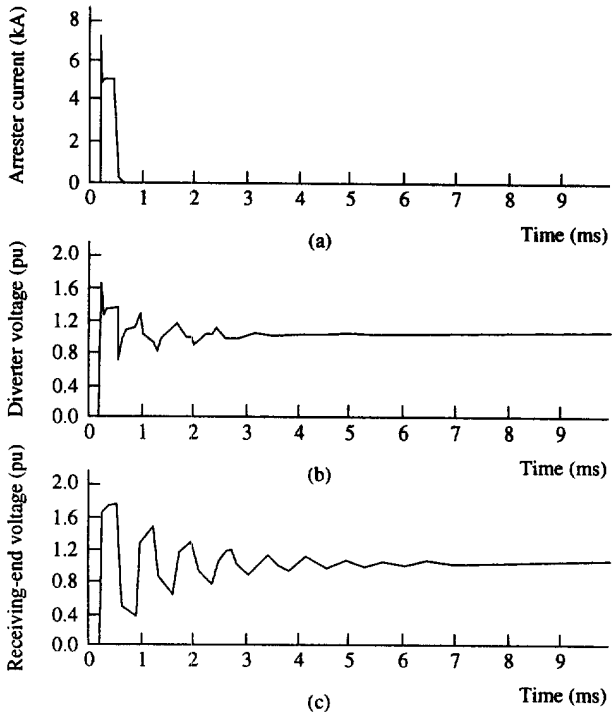

Fig. 10. The effect of surge divertor operation due to single-phase, unit step energisation of single-point bonded cable. (a),(b) Response of the surge divertor, (c) receiving end voltages (no divertors). ____ energised phase (phase 1).

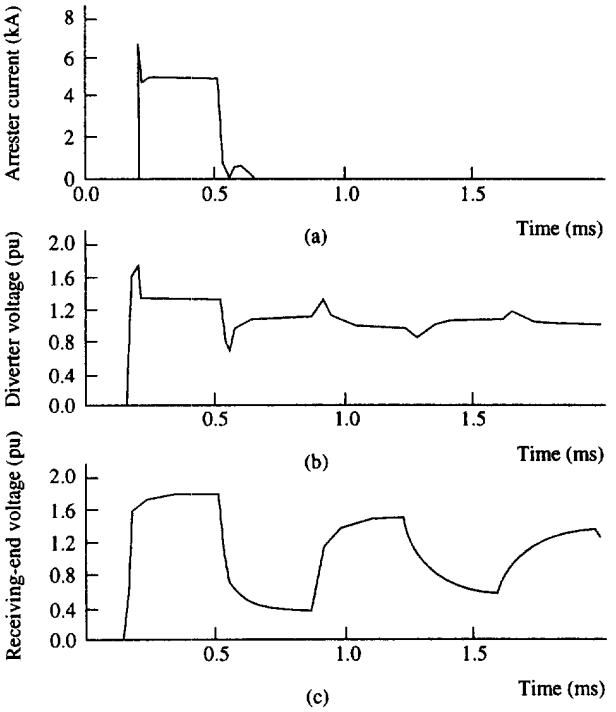

Fig. 11. The effect of surge divertor operation due to single-phase, unit step energisation of single-point bonded cable (observation time—2 ms). (a),(b) Response of the surge divertor, (c) receiving end voltages (no divertors). ____ energised phase (phase 1).

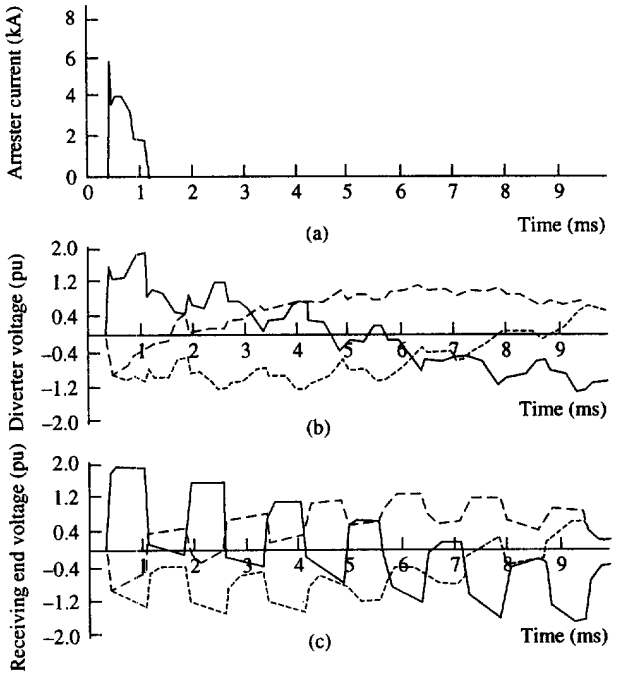

Fig. 12. The effect of infinite bus-bar source upon the divertor operation. (a),(b) Response of the surge divertors, (c) receiving end voltages (no divertors). ____ phase 1; · · · · · phase 2; – – – phase 3.

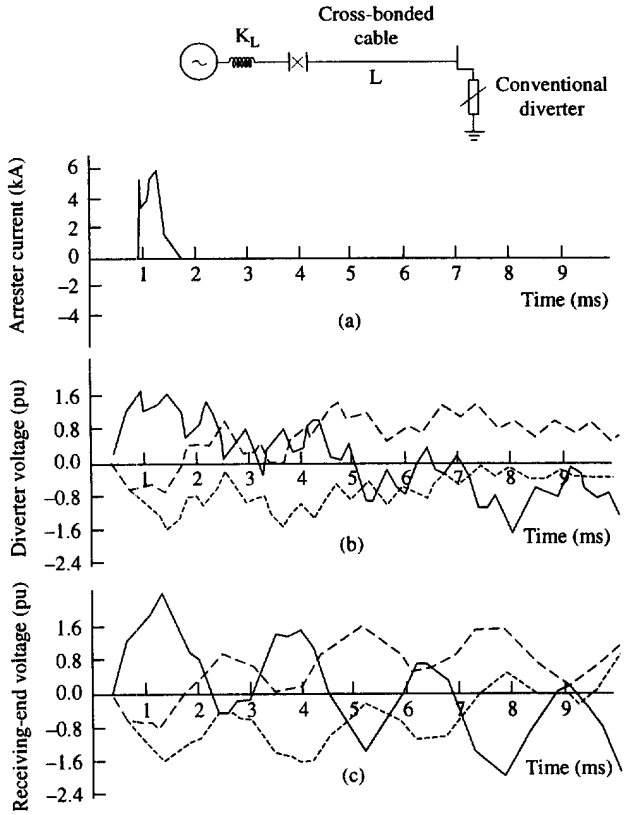

Fig. 13. The effect of a source of 0.012 henry (20,000 MVA) upon the divertor operation. (a),(b) Response of the surge divertors, (c) receiving end voltages (no divertors). ____ phase 1; · · · · · phase 2; – – – phase 3.

On the other hand, while the divertor is operating, it conducts a current, shown by Fig. 12a, which rises to a value of 6.45 kA sharply and flows for a time of 1.16 ms.

Contrary to the infinite busbar source, inductive sources cause the initial voltages to rise exponentially. The voltage waveforms at the divertor location with and without active-gap surge divertors being present are given by Figs 13–16 for various source conditions (X_L = 12, 16.1, 24.1 and 42.5 mH, respectively), i.e. for different short-circuit fault levels in each case. The rate of rise of the voltage wavefront decreases when the source inductance gets bigger and bigger. After each divertor sparkover, the voltages at the divertor location are modified, and high frequency oscillations take place. In some other cases, however, simultaneous operations of surge divertors take place as can be seen in Fig. 16a. In each of these cases, surge divertor currents rise as high as 6 kA.

Figure 17 shows the responses for the case of a mixed source, i.e. an inductance (X_L = 42.5 mH) in series with a resistance (R = 6.68 Ω). The resistance value is chosen to give a Q factor ($Q = \omega I/R$) of 10 at a frequency of 250 Hz. If Fig. 17c is compared with Fig. 16c, it is seen that the effect of introducing such a series resistance is to damp the voltages slightly at the divertor location and also to suppress simultaneous divertor operations.

6.2.2. Effect of cable length. The total length, i.e. number of major sections, of a cross-bonded cable consisting of several major sections is an important factor affecting the divertor performance. To illustrate this, cross-bonded cables with different numbers of major sections, such as 5, 10, and 15, are considered. Each major section has a length of 1.371 km. The responses are obtained using a maximum frequency harmonic of 10 kHz.

The effect of cable length is illustrated by Figs 12 and 18–20 (L = 20.574, 13.716 and 6.858 km, respectively). It can be seen from these figures that the receiving end voltage waveforms with no divertors are oscillatory. The frequency of oscillations increases as the cable length is decreased, however the voltage peaks remain the same. For the cable length of 27.432 km (20 major sections), the frequency of oscillations is 667 Hz, whereas it is 874 Hz for 20.574 km (15 major sections), 1273 Hz for 13.716 km (10 major sections), and 2667 Hz for 6.858 km (five major sections) of cable. It may be observed that the frequency of oscillations is quite high, particularly for the cable length of five major sections.

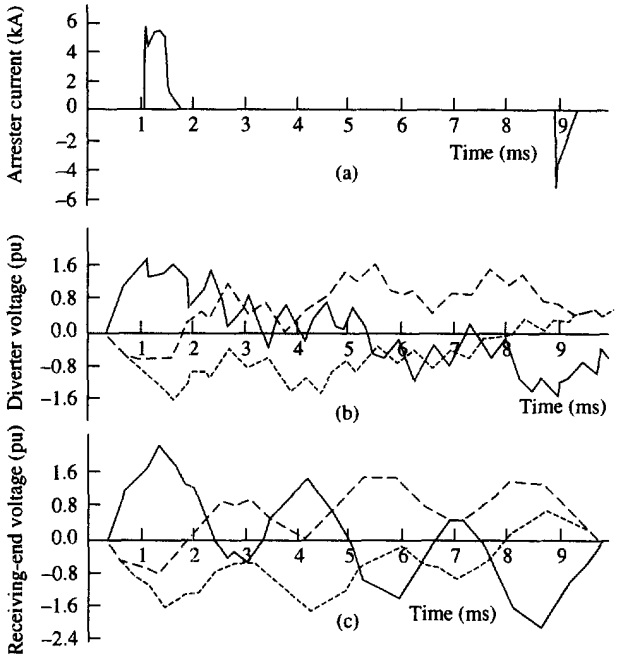

Fig. 14. The effect of a source of 0.0161 henry (15,000 MVA) upon the divertor operation. (a),(b) Response of the surge divertors, (c) receiving end voltages (no divertors). ___ phase 1; ····· phase 2; – – – phase 3.

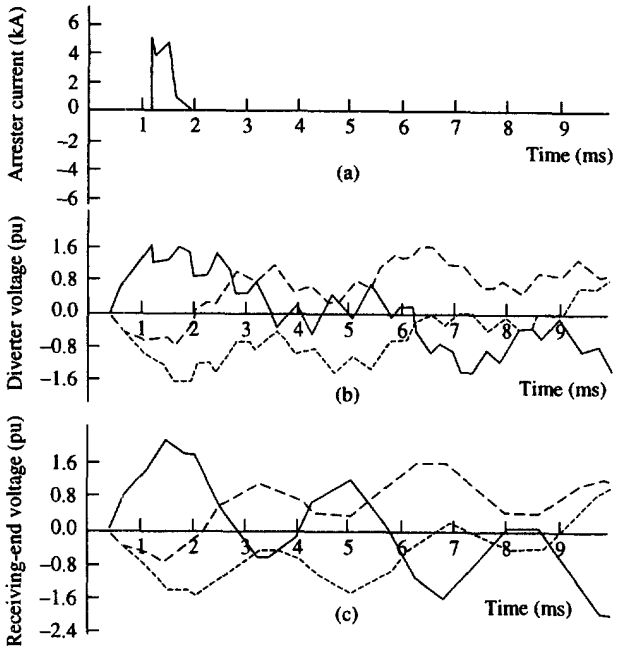

Fig. 15. The effect of a source of 0.0241 henry (10,000 MVA) upon the divertor operation. (a),(b) Response of the surge divertors, (c) receiving end voltages (no divertors). ____ phase 1; · · · · · phase 2; – – – phase 3.

The operations of surge divertors also modify the receiving end voltages, depending on the cable length. It may be seen from Figs 12b and 18b–20b that the modified voltage waveforms have also oscillations, the frequencies of which are almost the same as the corresponding frequencies given

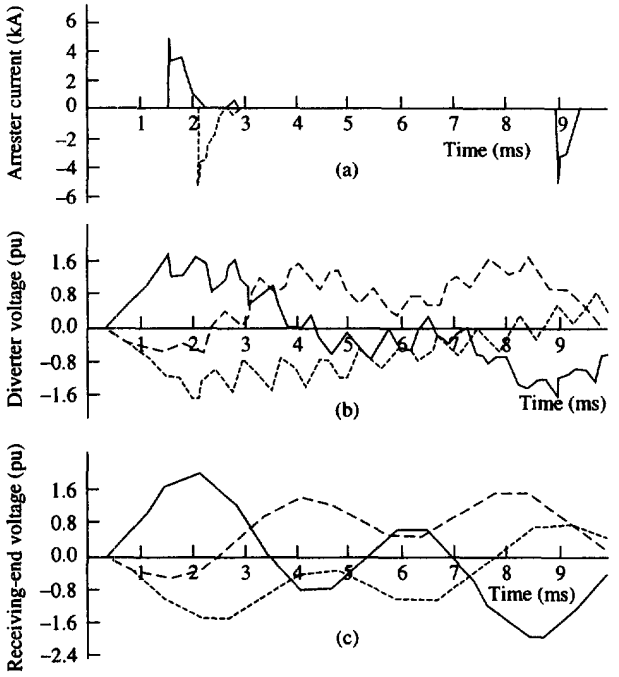

Fig. 16. The effect of a source of 0.0425 henry upon the divertor operation. (a),(b) Response of the surge divertors, (c) receiving end voltages (no divertors). ____ phase 1; · · · · · phase 2; – – – phase 3.

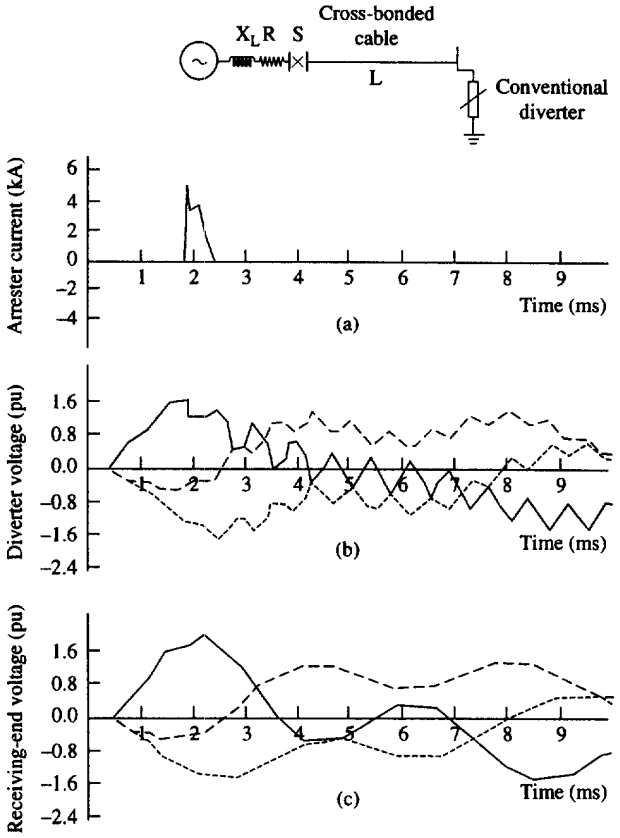

Fig. 17. The effect of a mixed source having an inductance of 0.0425 henry in series with 6.68 ohms, upon the divertor operation. (a),(b) Response of the surge divertors, (c) receiving end voltages (no divertors). ____ phase 1; · · · · · phase 2; – – – phase 3.

above. Sparkover of a divertor affects all the phase voltages, that is, each phase voltage is modified under the effect of every sparkover.

The currents flowing through the operated divertors have different shapes depending on the cable lengths, but maximum values reach almost 6 kA in each case.

6.2.3. Effect of sheath earthing-resistance. The effect of sheath earthing-resistance has been studied for the cases: sheaths earthed solidly and sheaths earthed through resistors of 5 Ω or 10 Ω. The cross-bonded cable having a total length of 27.432 km is energised from an infinite bus-bar.

It has been observed from the results that the voltages induced on the sheaths are negligible for the sheath earthing conditions studied. The magnitudes of the receiving end voltages corresponding to each phase are not influenced by the sheath earthing-resistance.

The voltage responses of the divertors have similar waveforms. The maximum values of the divertor currents, however, are reduced as the sheath earthing-resistance is increased. This may be seen from Table 1. The operation periods of the divertors are around 1.1 ms.

6.2.4. Effect of cable type. The responses of conventional active-gap surge divertors are obtained for cross-bonded and single-point bonded cables and compared with each other. Both types of cable systems, which have identical cable parameters, dimensions and conductor spacings, are energised from infinite bus-bars. The maximum frequency harmonic considered is 15 kHz.

In the case of the cross-bonded cable, the responses of the divertor have been given in Fig. 12. In the case of the single-point bonded cable, however, the divertor response is obtained, as shown in Fig. 21. It is seen from this figure that the voltage and current of the operated divertor are similar to those obtained by the single-phase energisation. Hence, the comments relevant to the case of single-phase energisation mentioned in the previous sub-section apply to the case of three-phase energisation as well, so as to compare the divertor responses in different cable types. It may be

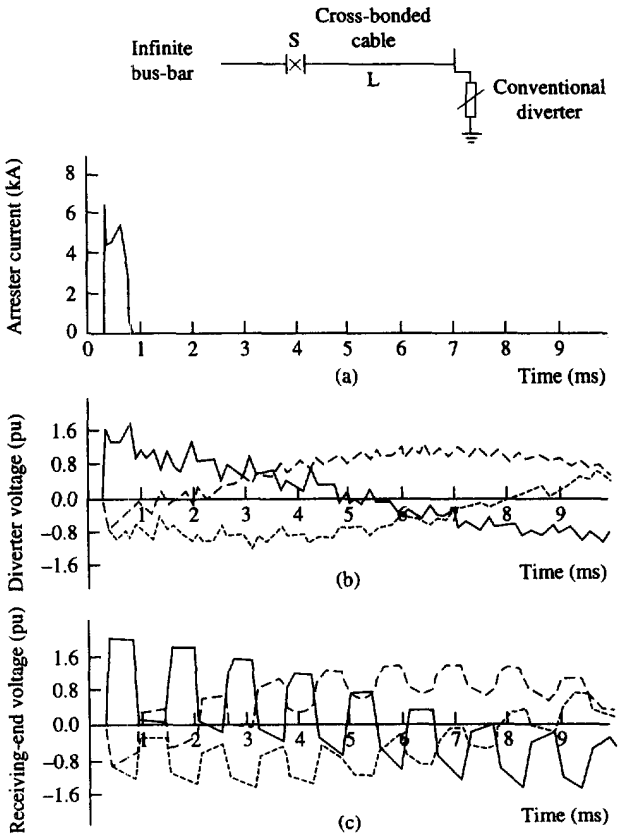

Fig. 18. Effect of cable length: $l = 20.574$ km (15 major sections). (a),(b) Response of the surge divertors, (c) receiving end voltages (no divertors). ___ phase 1; · · · · · phase 2; – – – phase 3.

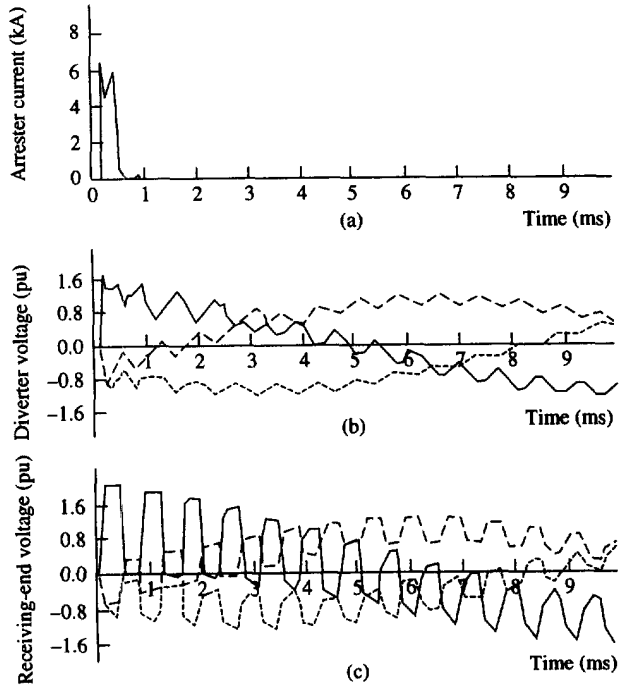

Fig. 19. Effect of cable length: $l = 13.716$ km (10 major sections). (a),(b) Response of the surge divertors, (c) receiving end voltages (no divertors). ___ phase 1; · · · · · phase 2; – – – phase 3.

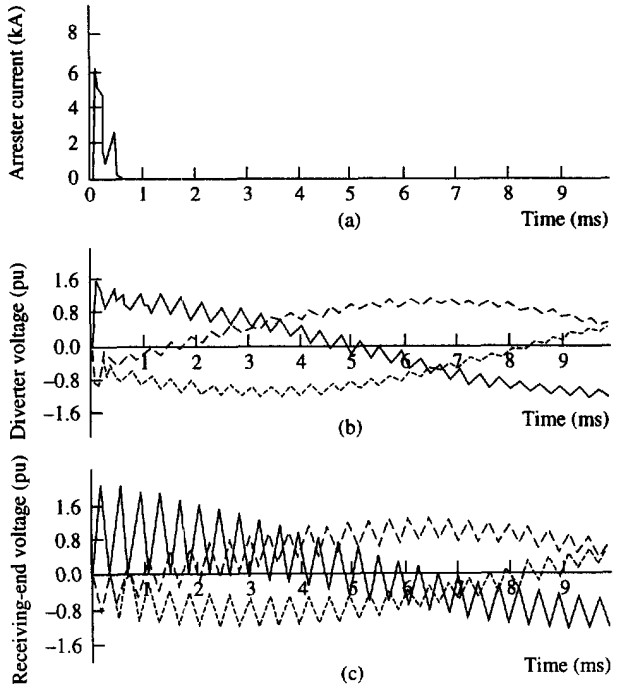

Fig. 20. Effect of cable length: $l = 6.858$ km (five major sections). (a),(b) Response of the surge divertors, (c) receiving end voltages (no divertors). ___ phase 1; · · · · · phase 2; – – – phase 3.

seen from Fig. 21 that the mutual effects between phases due to the operation of the surge divertor on phase 1 are negligible in the case of the single-point bonded cable. On the other hand, considerable voltage modifications appear on the phase on which the surge divertor sparks over.

6.2.5. Effect of divertor type. The non-linear characteristic of a surge divertor, because of its non-linear valve resistors as well as, if it exists, its spark-gaps, is an important factor in the modification of system voltages. In particular, the non-linear characteristic of a gapless surge divertor is quite different from that of a conventional divertor because of the fact that no spark-gaps exist in series with its non-linear resistors, and its non-linearity is further improved to provide a better protective characteristic. On the other hand, gapless divertors do not possess any distinct sparkover voltage levels due to the lack of the spark-gaps. This also has an effect on the modification of system voltages during the operation of the divertors.

In order to get a clear idea about the effects of surge divertor type, conventional active-gap and gapless divertors are considered in the studies. Both types of divertors are employed in cross-bonded and single-point bonded cable systems separately, and the results are compared with one another. Figures 22 and 23 (for infinite bus-bar source) show the responses of gapless surge divertors for the cases of single-point bonded and cross-bonded cable systems, respectively. If these are compared with the corresponding responses of conventional surge divertors shown in Figs 12 and 21, it is seen that, in the case of gapless surge divertors, the voltage responses are smoother compared to those obtained in the case of conventional divertors because sparkover transients do not occur when gapless divertors operate. On the other hand, so far as the maximum values of the divertor currents are concerned, gapless divertors draw currents of smaller maximum values

Table 1. Variation of divertor currents with sheath earthing-resistance of the cable

Sheath earthing-resistance (Ω)	Maximum current of the operated divertor (kA)	Operation period of the divertor (ms)
0	6.453	1.16
5	6.049	1.13
10	5.824	1.13

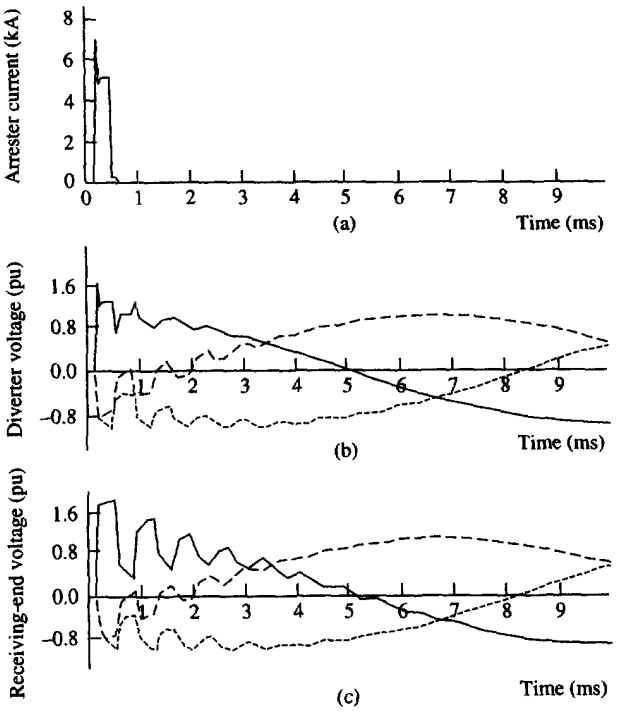

Fig. 21. Effect of active-gap divertor on single-point bonded cable system. (a),(b) Response of the surge divertors, (c) receiving end voltages (no divertors). ____ phase 1; ····· phase 2; – – – phase 3.

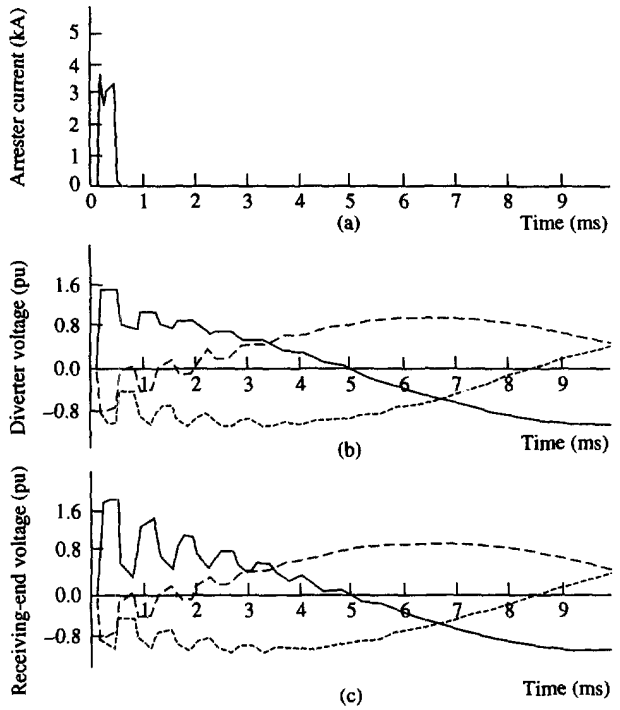

Fig. 22. Effect of gapless surge divertor on single-point bonded cable system. (a),(b) Response of the surge divertors, (c) receiving end voltages (no divertors). ____ phase 1; ····· phase 2; – – – phase 3.

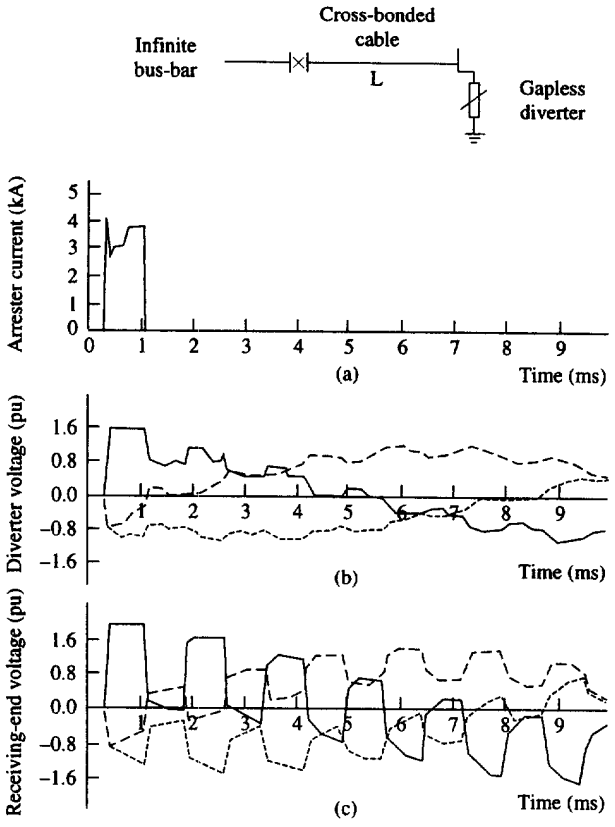

Fig. 23. Effect of gapless surge divertor on cross-bonded cable system. (a),(b) Response of the surge divertors, (c) receiving end voltages (no divertors). ____ phase 1; ····· phase 2; – – – phase 3.

compared to the others, as can be seen from the figures. It is seen from the results obtained that gapless surge divertors are preferable in cable circuits compared to the conventional types due to their better performance against severe surges, such as against those which have steep wavefronts, and also due to their ability to draw small-magnitude discharge currents.

7. CONCLUSIONS

The present work is concerned with studying the effects of including divertors, as one of the non-linear protective devices, for the protection of electrical power cable systems, under energisation conditions.

The study shows that the energisation of a cable system produces transient voltages sufficient to operate the divertors at the receiving ends. It has been shown that the operation of divertors can control such switching surges to some extent.

The approach to include the non-linear effects of surge divertors gives satisfactory results, as verified in this study. The computer results obtained are in very good agreement with those given by Sakshaug *et al.* [16].

The divertor operation modifies the system voltages under the effects of various system parameters and divertor characteristics. The severity of discharge duty of divertors is a function of the surge impedance of the cable system and the series divertor impedance. Cable circuits increase the discharge duty imposed upon divertors because of low surge impedance and increased capacitance per unit length of cable. Because of the capacitive effect of the cable and high energy being stored in it, divertor sparkover causes the discharge current of the divertor to rise sharply.

When divertors are placed at the receiving end of the cable, the source inductance and cable length do not have much effect on the maximum magnitudes of divertor currents. The maximum magnitude of the discharge current, in the case of the cross-bonded cable, is almost 6 kA. The divertor current rises to this value abruptly with a steep wavefront. Depending on the system parameters, e.g. source impedance, system length, etc. the number of divertor sparkovers varies, and multiple simultaneous operations might take place. The series source resistance damps the divertor voltages slightly and eliminates any simultaneous divertor operations.

As the sheath earthing-resistance of the cross-bonded cable is increased, the divertor discharge current gets smaller.

The behaviour of surge divertors at the receiving end of a single-point bonded cable is such that the divertor voltage, after sparkover, comes to the steady-state value much more quickly than that in the case of the cross-bonded cable. The divertor current rises to a higher maximum value, which is about 7 kA, because the single-point bonded cable has a smaller surge impedance than the cross-bonded cable, both having the same cable parameters and dimensions.

As far as the performance of recently developed gapless divertors are concerned, they provide superior protective characteristics compared to conventional divertors. During their operation, the cable system is not subjected to sparkover transients, since the valve elements enter into conduction smoothly. This, however, is due to the absence of the spark-gaps within these divertors. Therefore, operations of gapless divertors do not modify the system voltages much. The currents flowing through them during operation are quite small in magnitude, as compared with those flowing through conventional divertors. The behaviour of gapless divertors under energisation conditions has shown that they can provide fairly satisfactory protection against switching overvoltages.

REFERENCES

1. Price, W. S., McElroy, A. J., *et al. IEEE Transactions*, 1956, **75,** 481.
2. Abdel-Gawad, N. M. K. Analysis of non-linearities in cross-bonded cable systems, *Al-Azhar Engineering 4th International Conference*, Cairo, Egypt, 1995.
3. Phelps, J. D. M., Pugh, P. S. and Beehler, J. E. *IEEE Transactions*, 1969, **PAS-88,** 1377.
4. Frey, W. and Althammer, P. *Brown Bov. Rev.* 1961, **48**(5/6), 344.
5. McElroy, A. J. and Porter, R. M. *IEEE Transactions*, 1963, **PAS-82,** 88.
6. Thoren, B. and Carlsson, L. *IEEE Transactions*, 1970, **PAS-89**(62), 212.
7. Dommel, H. W. *IEEE Transactions*, 1971, **PAS-90,** 2561.
8. Schei, A. and Johansson, A. Temporary overvoltages and protective requirements for EHV and UHV arresters, CIGRE, Paris, 1972, Report 33-04.
9. Sakshaug, E. C. *et al.* Requirements on EHV and UHV surge arresters, comparison of energy and current duties between field and laboratory conditions by means of TNA simulation, CIGRE, Paris, 1976, Report 33-10.
10. Carrara, G., Clerici, A. *et al. IEEE Transactions*, 1969, **PAS-88**(10), 1449.
11. Taylor, Jr., E. R. and Merry, S. M. *IEEE Transactions*, 1971, **PAS-90,** 1103.
12. Ozaki, Y. *et al.* New concepts on overvoltage protection by surge arresters, CIGRE, Paris, 1978, Report 33-02.
13. Hieda, S. *et al. Meiden Rev.* 1975, **2** Pt. 46, 17.
14. Aleksandrov, G. N. *et al.* Arresters for substantial limitation of overvoltages in 110–500 kV electric systems, CIGRE, Paris, 1978, Report 33-06.
15. Kobayashi, M. *et al. IEEE Transactions*, 1978, **PAS-97**(4), 1149.
16. Sakshaug, E. C. *et al. IEEE Transactions*, 1977, **PAS-96**(2), 647.
17. Wedepohl, L. M. and Mohamed, S. E. T. *Proceedings of the IEE*, 1973, **120,** 253.
18. Guillemin, E. A. *Theory of Linear Physical Systems*, John Wiley & Sons, New York, 1963.
19. Wylie, C. R. *Advanced Engineering Mathematics*, McGraw-Hill, New York, 1975.
20. Greenwood, A. *Electrical Transients in Power Systems*, John Wiley and Sons, New York, 1971.
21. Ametani, A. *Proceedings of the IEE*, 1973, **120**(4), 497.
22. Ametani, A. *IEEE Transactions*, 1976, **PAS-95**(5), 1545.
23. Wasley, R. G. *IEEE Transactions*, 1977, **PAS-96**(1), 248.

APPENDIX

1. *Appendix A: Data used for the studies*

Table A1. Cable data

Conductor radius	1.969 cm
Sheath inner radius	3.556 cm
Sheath outer radius	3.708 cm
Cable outer radius	4.115 cm
Resistivity of core	1.72×10^{-8} Ω-m
Resistivity of sheath	3.58×10^{-8} Ω-m
Relative permittivity of core insulation	3.72
Relative permittivity of sheath insulation	2.33
Relative permeability of the core	1.0
Relative permeability of the sheath	1.0

Table A2. Modal parameters of the 275 kV cross-bonded cable, the sheaths of which are solidly earthed at the major section joints (frequency = 50 Hz, earth resistivity = 20 Ω-m)

Major Section Characteristic Impedance Matrix Z_0 (Ω/deg)		
38.13/ − 11.42	6.70/ − 125.10	6.70/ − 125.10
6.70/ − 125.10	38.13/ − 11.42	6.70/ − 125.10
6.70/ − 125.10	6.70/ − 125.10	38.11/ − 11.42

Major Section Characteristic Admittance Matrix Y_0 (m Mho/deg)		
24.92/13.60	4.64/89.75	4.64/89.75
4.64/89.75	24.92/13.60	4.64/89.75
4.64/89.75	4.64/89.75	24.92/13.60

Mode No.	Eigen vectors		Velocity	Attenuation
	Voltage	Current	km/sec	dB/km
	1.0/0.0	0.50/0.0		
1	0.0/0.0	0.0/0.0	69411	0.00197
	1.0/180.0	0.50/180.0		
	0.50/180.0	0.333/180.0		
2	1.0/0.0	0.667/0.0	69411	0.01197
	0.50/180.0	0.333/180.0		
	1.0/0.0	0.333/0.0		
3	1.0/0.0	0.333/0.0	96469	0.01766
	1.0/0.0	0.333/0.0		

Table A3. Modal parameters of the 275 kV single-point bonded cable, the sheaths of which are solidly earthed at the terminating ends (frequency = 50 Hz, earth resistivity = 20 Ω-m)

Characteristic Impedance Matrix Z_0 (Ω/deg)		
34.6/ − 23.77	2.50/ − 113.61	2.50/ − 113.61
2.50/ − 113.61	34.60/ − 23.77	2.50/ − 113.61
2.50/ − 113.61	2.50/ − 113.61	34.60/ − 23.77

Characteristic Admittance Matrix, Y_0 (milli Mho/deg)		
28.61/23.73	2.06/118.02	2.06/118.02
2.06/118.02	28.61/23.73	2.06/118.02
2.06/118.02	2.06/118.02	28.61/23.73

Mode No.	Eigen vectors		Velocity	Attentuation
	Voltage	Current	km/sec	dB/km
	0.577/0.0	0.577/0.01		
1	0.577/0.0	0.577/0.0	96469	0.01766
	0.577/0.0	0.577/0.0		
	0.816/0.0	0.816/0.0		
2	0.408/180.0	0.408/180.0	87610	0.01112
	0.408/180.0	0.408/180.0		
	0.0/0.0	0.0/0.0		
3	0.707/180.0	0.707/180.0	87610	0.01112
	0.707/ 0.0	0.707/0.0		